DIGITAL IMAGERY AND GEOLOGIC MAP OF CHEGEM CALDERA, RUSSIA

Christina Cauley
Department of Geology and Anthropology
University of Hawai‘i at Hilo
Hilo, HI 96720

ABSTRACT

The late Pliocene Chegem Caldera in the North Caucasus, Russia, is the youngest, most deeply dissected, resurgent caldera complex in the world. The caldera system contains close to three kilometers of vertical exposure including the resurgent intrusion. Field mapping of this remarkable system, done during the summers of 1990 and 1991, remain unpublished and exist only on photographs of Russian topographic maps. The primary project goals were to register and digitize the maps onto a topographic base derived from an ASTER global DEM and to use multispectral imagery to confirm and extend the geologic mapping of this remote site. Most of the caldera lies above tree-line, making it well suited for satellite imaging. Utilizing data from the LANDSAT and ASTER satellites in conjunction with ground-based research conducted in 1990 and 1991, a publishable geologic map of the caldera was produced.

INTRODUCTION

The Chegem Caldera complex is notable not only for containing a diverse number of units but also for the degree of down cutting that makes the complex the youngest, most deeply dissected, resurgent caldera in the world. The current size of Chegem Caldera is 11 x 15 km in diameter. The original topographic size of the Chegem caldera was on the order of 15 x 20 km, with outflow sheets extending at least 40-50 km from the caldera margins. Intra-caldera ash-flow tuffs are more than two kilometers thick within the source caldera (Lipman et al. 1993).

The Chegem Caldera complex was active 2.8 million years ago during the late Pliocene continental collisional event between the northward moving Arabian plate and Eurasian plate (Lipman et al. 1993, Gazis et al. 1995). Recent rates of uplift in the Northern Caucasus are as great as four millimeter per year, which along with denudation has resulted in a 2.3 km thick section of caldera fill to be exposed in deeply dissected river drainages (Lipman et al. 1993, Gazis et al. 1995). The region is surrounded by thrust and reverse faults, along with trending transverse faults in the northeast zone of the caldera. Four sequential orogenic belts are co-located around the Chegem caldera system (Lipman et al. 1993).

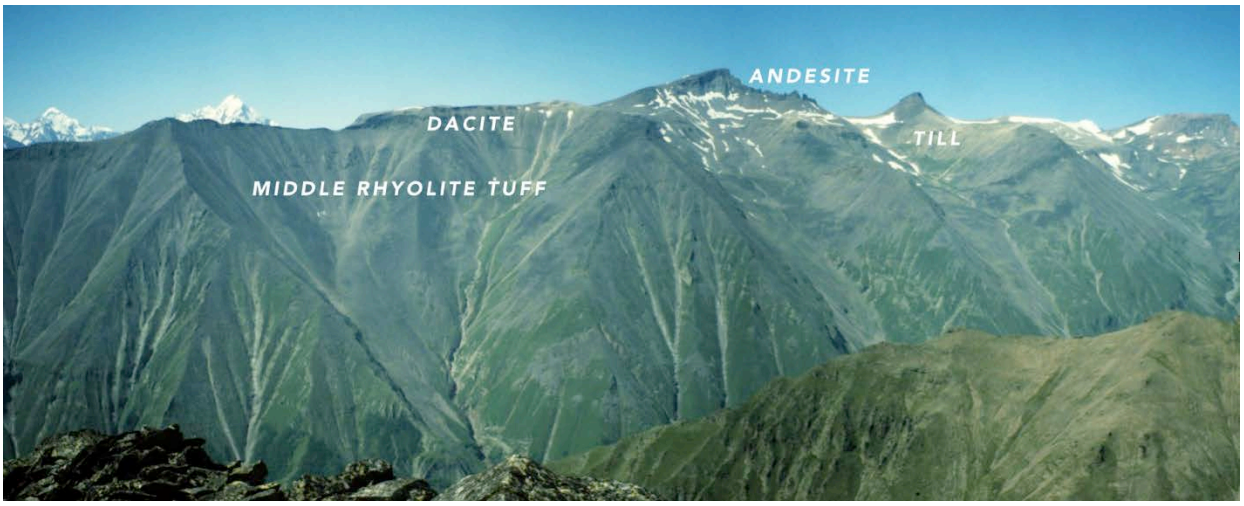

Figure 1: The Kum Tyube section of the thick rhyolitic tuffs capped by dacite tuffs, glacial till and andesite lavas. Photo taken from Mt. Likarilgi, facing the southwest, by Dr. Ken Hon in 1991.

A variety of volcanic and intrusive events have formed a compositionally diverse suite of units, including basaltic andesites, andesites, granodiorites, granites, and welded and nonwelded dacite and rhyolite tuffs. These overlay Jurassic- Cretaceous sedimentary rocks and Precambrian to Paleozoic crystalline basement rocks that are predominantly schists. Glacial till has been deposited on both within and on top of these sequences and fossil talus breccia was identified in the caldera collapse features. The intra-caldera ash-flow sequences are characterized by the absence of complete cooling breaks or other evidence for interruptions in deposition. The southeastern portion of the caldera complex was shaped by simple piston uplift of a resurgent block. Overall, the whole mass appears to have formed over a period of less than 50,000 years (Lipman et al. 1993, Gazis et al. 1995, 1996).

The field conditions in the Chegem Caldera region are extremely rugged and in places not conducive to fieldwork. Portions of the contacts between units remained poorly constrained due to difficulty accessing the contact in the field, especially the northern and western regions. Additionally, the glacial meltwaters of the Chegem River and its tributaries make crossings hazardous (Lipman et al. 1993). A geologic map for the caldera was compiled from pre-existing topographic maps and mapping done by a joint Russian Akademia NAUK and U.S. Geological Survey team lead by Peter Lipman during the summers of 1990 and 1991. The map remains unpublished, with regions of uncertainty where the landscape was not traversable. Current social conflicts in the area make future fieldwork in the region difficult. The application of remote sensing imagery was done in an effort to refine the geologic map structures and contacts where possible in light of these physical restrictions in access to the area as well as to produce a digital map with a rectified topographic base.

METHODS

A LANDSAT 7 EMT+ image and two ASTER Global digital elevation models (DEM) were procured and processed. These datasets were essential to geo-registering and transforming the original geologic maps to an accurate topographic base.

The DEM datasets and the Landsat image were processed in ENVI and ArcGIS. The ASTER DEMs used were collected in October 201l. No other ASTER data then DEMs were availed online for this region. The two DEM were reprojected, mosaicked and cropped. The mosaicked DEM then imported into ArcGIS and used to produce 100 m and 200 m topographic lines. The resulting DEM was processed in ArcHydro to generate an accurate stream drainage system. A network of points identifiable on the original map, the stream drainage map, the Landsat image, and 1 m satellite imagery available within ENVI were chosen.

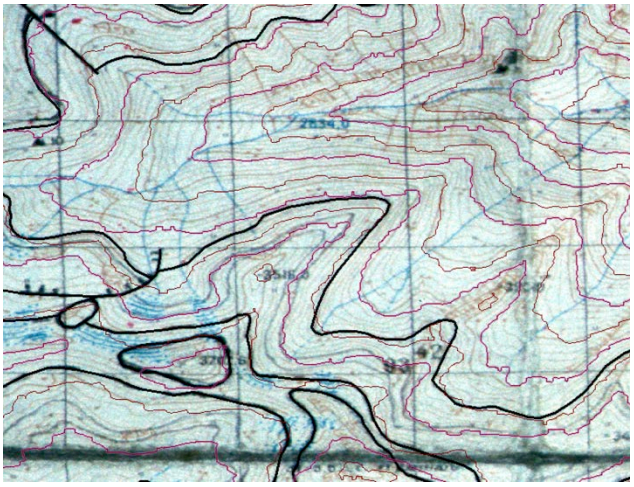

Figure 2: The high degree of agreement between the ASTER derived contour lines and the topographic map contours assured the geo-rectification of the base maps was accurate. NASA ASTER Program (2011).

The completed ArcGIS feature classes drew from a total of ten map images. Creating a stable topographic base to insure the alignment of the field and satellite data was crucial as this provided the backbone for my analysis. The topographic maps were initially geo-rectified using 44 manually created control points that were identifiable in all three data sets, then further refined by registering points at the edge of one image to the same point in another. By comparing the map elevation contour lines against the independently created contour lines from the ASTER DEM the accuracy of the geo-rectified map was tested. The high degree of agreement between the data assured that transformed base was accurate. The best-fit for the entire map had to be tested and the results considered when defining the primary geologic contacts.

The LANDSAT 7 EMT+ image was taken in August 1999. The image was cropped, Gram-Schmidt pan sharpening and a QUAC atmospheric correction was applied. Several decorrelation stretches have been applied to the LANDSAT images to enhance the visual differences between the geologic units. The stretches were done using band combinations 754, 542, and 731. These combinations were elected to make use of three key bands. The short wave length IR bands 7 and 5 are useful for general mineral and rock discrimination. The near IR band 4 provided an accurate delineation of vegetation covered. Once the map contacts were matched to units visible in the LANDSAT image, the spectral signature of each unit was calculated.

RESULTS AND DISCUSSION

The spectral signatures of the volcanic units were distinct from those of the limestone and glacial till (Fig. 3). There is a significant amount of overlap between the volcanic and intrusive units within the caldera and plots demonstrated that they were highly correlated. Several decorrelation stretches were applied that accurately discriminated most of the mapped units on

the Landsat image. Attempts at classification were hampered by shadowed regions in deep valleys, large amounts of talus that bleed the contacts downhill, and by dense vegetation particularly in the valleys. Even so, most of the geologic units were clear in the decorrelated images. In particular, the decorrelated stretches were successful in highlighting the resurgent intrusion, the hornfelsed tuff in the resurgent block, and large areas of potential tuff plastered against the topographic caldera wall outside the structural caldera that were not identified in the field.

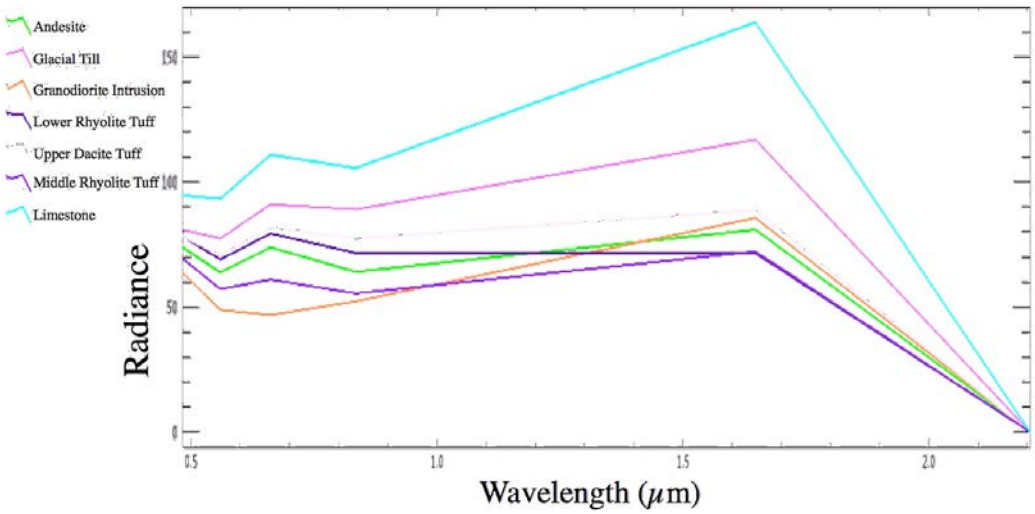

Figure 3: Spectral signatures of the limestone and igneous geologic units. NASA Landsat Program (1999).

Glacial till deposits were readily identifiable in the LANDSAT image, which we had initially assumed would be the most difficult unit to identify spectrally due to the mixed composition. It appears to be composed predominantly of limestone parent material, which clearly delineates the glacial till from the surrounding igneous deposits.

In the red and infrared bands, the granodiorite intrusion and the lower rhyolite tuff were clearly delineated from all other units. Contact metamorphism from the intrusion of the granodiorite caused the partial melting and recrystallization of the tuff into hornfels created the unique spectral signature of this unit. The LANDSAT images clearly support the field team's initial inferences about the overall structure as the fault bounding of resurgent block in the northeast section of Chegem Caldera. Much of area of the resurgent block lies in inaccessible terrain, so the confirmation of the geology from the remote sensing data is extremely valuable.

Vegetation cover was a larger issue in the northeast region of Chegem Caldera then we had assumed it would be at the start of the project. The hornfelsed lower rhyolite tuff identified in the field on the Hobetayeen mountain block was not detectible in the LANDSAT image. This was largely due to extensive grass, brush, and trees in this area. The unit extent was determined based upon the original field notes and the size limits from the surrounding granodiorite unit, decreasing the extent of this unit compared to the original geologic maps.

CONCLUSIONS

Ten geologic maps were accurately geo-rectified and compiled into a single digital map. This allows for the successful use of satellite imagery to confirm geologic units and the structure of the caldera system. This includes the shape of the resurgent block, as well as several large areas of potential Chegem tuff outside of the structural margins. Future work in this region would include analyzing a larger footprint of the area to identify the geographic extents of the ash flow sheets described by Lipman et al. in 1993.

ACKNOWLEDGEMENTS

Many thanks to my mentor, Dr. Ken Hon, for giving me this opportunity and providing the topographic maps for this project. I would also like to thank Dr. Ryan Perroy for introducing me to ENVI, and to the University of Hawai‘i at Hilo for access to the software used in this project.

REFERENCES

Adamia S., Zakariadze G., Chkhotua T., Sadradze N., Tsereteli N., Chabukiani A., and Gventsadze A. (2011). Geology of the Caucasus: A Review. Turkish J. Earth Sci. 20, 489–544.

Gazis C. A., Lanphere M., Taylor H. P., and Gurbanov A. (1995). 40Ar/39Ar and 18O/16O studies of the Chegem ash-flow caldera and the Eldjurta Granite: Cooling of two late Pliocene igneous bodies in the Greater Caucasus Mountains, Russia. Earth Planet Sci. Lett. 134, 377–391.

Gazis C., Taylor H. P., Hon K., and Tsvetkov A. (1996). Oxygen isotopic and geochemical evidence for a short-lived, high-temperature hydrothermal event in the Chegem caldera, Caucasus Mountains, Russia. J. Volcanol. Geotherm. Res. 73, 213–244.

Hon K. (Photographer) (1991). Kum Tyube Ridge, Chegem Caldera, Russia [photograph]. Private Collection.

Lipman P. W., Bogatikov O. A., Tsvetkov A. A., Gazis C., Gurbanov A. G., Hon K., Koronovsky N. V., Kovalenko V. I., and Marchev P. (1993). 2.8-Ma ash-flow caldera at Chegem River in the northern Caucasus Mountains (Russia), contemporaneous granites, and associated ore deposits. J. Volcanol. Geotherm. Res. 57, 85–124.

NASA ASTER Program (2011). ASTER Global DEM scene, ASTERGDMV2_0N43E042, USGS, Sioux Falls, 10/17/2011.

NASA ASTER Program (2011). ASTER Global DEM scene, ASTERGDMV2_0N43E043, USGS, Sioux Falls, 10/17/2011.

NASA Landsat Program (1999). Landsat 7 EMT+ scene, L71171030_03019990818, level-1G, SLC-On. USGS, Sioux Falls, 08/08/1999.

Chegem Caldera, Russia

Christina Cauley, Mentor: Dr. Ken Hon

Reference Scale: 1:100,000

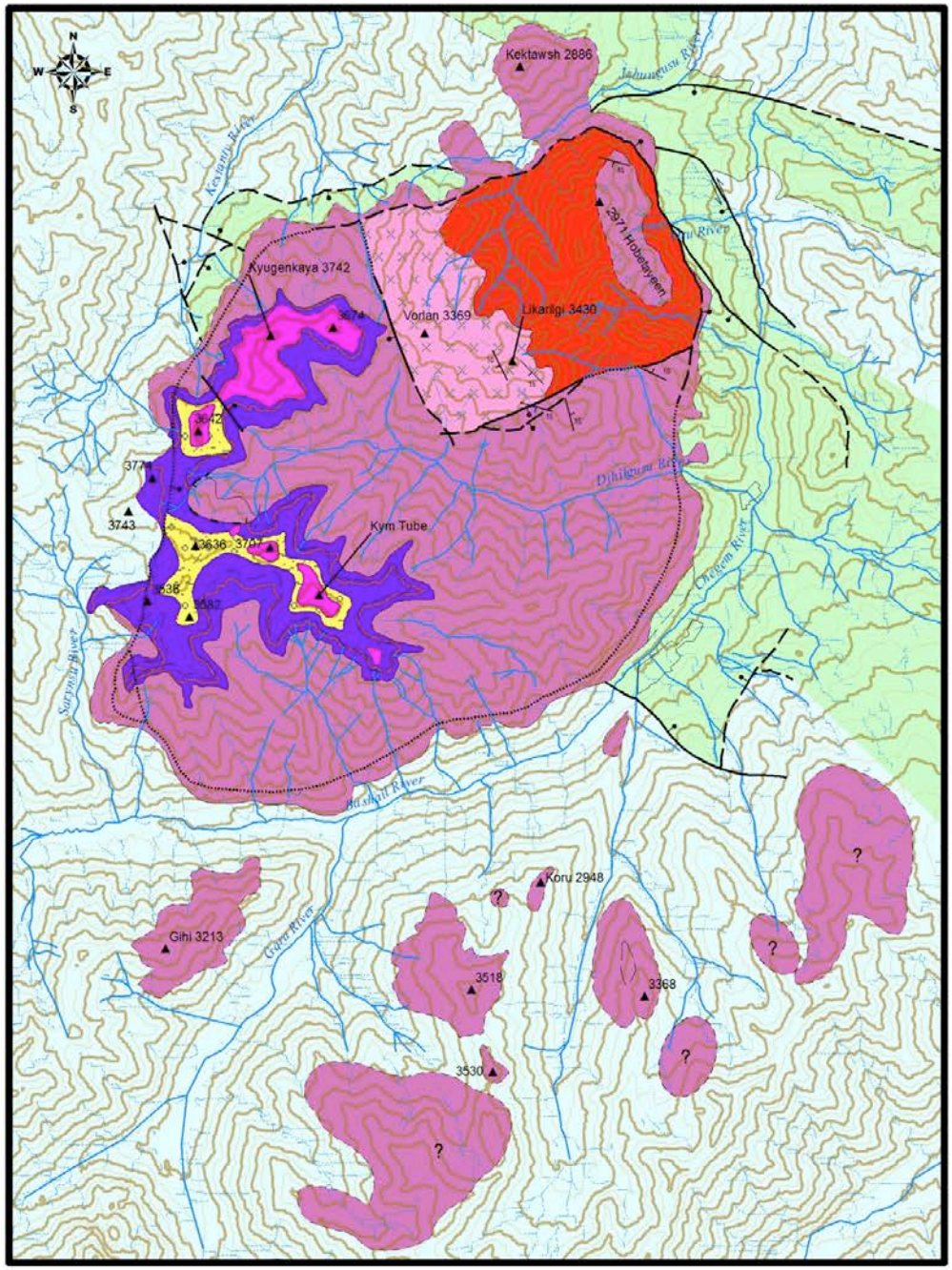

Legend

Geologic Units

- Andesite Flows
- Glacial Till
- Granodiorite Intrusion
- Upper Dacite Tuff
- Middle Rhyolite Hornfel Tuff
- Middle Rhyolite Tuff
- Lower Rhyolite Hornfel Tuff
- Jurassic-Cretaceous Sedimentary Rocks
- Precambrian & Paleozoic Crystalline Rocks

- Contact Certain
- Approximate Contact
- Contact Inferred
- Approximate Sub-unit Contact
- Fault Certain
- Approximate Fault
- Fault Concealed
- Normal Fault
- Approx. Located Normal Fault
- Normal Fault Concealed
- Scarp
- River
- 100 m Contour
- 200 m Contour
- ▲ Mt. Peak
- ? Identified from satellite data

Kilometers

5 2.5 0 5

Coordinate System: WGS 1984 UTM zone 38N
Projection: Transverse Mercator

ASTER DEM Derived Contour Intervals
Oct. 2011
NASA Landsat Program (1999)
NASA ASTER Program (2011)

Chegem Caldera, Russia

Christina Cauley, Mentor: Dr. Ken Hon

Reference Scale: 1:100,000

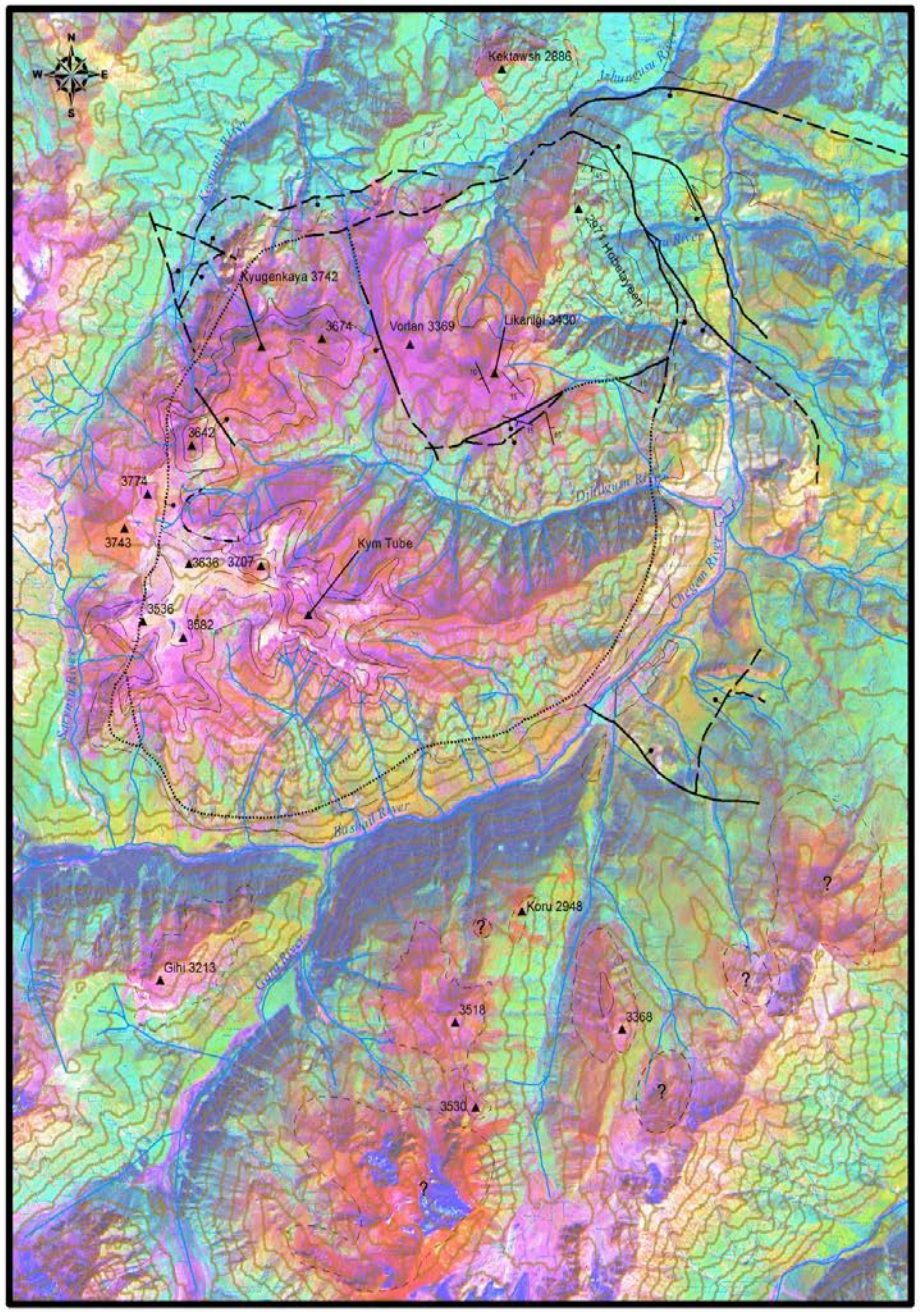

LANDSAT 7 EMT+ 754 Decorrelation Streach Image

Legend

Geologic Units

- Andesite Flows
- Glacial Till
- Granodiorite Intrusion
- Upper Dacite Tuff
- Middle Rhyolite Hornfel Tuff
- Middle Rhyolite Tuff
- Lower Rhyolite Hornfel Tuff
- Jurassic-Cretaceous Sedimentary Rocks
- Precambrian & Paleozoic Crystalline Rocks

- Contact Certain
- Approximate Contact
- Contact Inferred
- Approximate Sub-unit Contact
- Fault Certain
- Approximate Fault
- Fault Concealed
- Normal Fault
- Approx. Located Normal Fault
- Normal Fault Concealed
- Scarp
- River
- 100 m Contour
- 200 m Contour
- ▲ Mt. Peak
- ? Identified from satellite data

Kilometers

5 2.5 0 5

Coordinate System: WGS 1984 UTM zone 38N
Projection: Transverse Mercator

ASTER DEM Derived Contour Intervals
Oct. 2011
NASA Landsat Program (1999)
NASA ASTER Program (2011)